Iranian Journal of Chemical Engineering
Vol. 16, No. 4 (2019), IAChE

CFD Simulation of Methane Steam Micro-Reformer: Channel Design and Inlet/Outlet Configuration

H. Mohammadnezami, A. Irankhah [*]

Hydrogen and Fuel Cell Research Laboratory, Department of Chemical Engineering, Faculty of Engineering, University of Kashan, Kashan, Iran

ARTICLE INFO

Article history:
Received: 2019-08-18
Accepted: 2020-04-07

Keywords:
Micro-Reformer,
Channel Design,
Methane,
Simulation,
Fluent

ABSTRACT

Micro-reformers used for producing hydrogen with a high surface-to-volume ratio in small-scale fuel cells were investigated. To this end, scrutinizing and exploiting all areas of micro reformers is very important. Parallel micro-channels have shown good performance in eliminating dead volumes. Inlet/outlet configuration has great effect on the velocity distribution through micro-channels. In this study, four configurations (1 inlet/1 outlet on the same and opposite sides; 1 inlet/2 outlets on the same and opposite sides) were studied through simulation and 1 inlet/2 outlets on opposite sides were found to have the lowest velocity difference, hence having the best configuration. Simulations were carried out at 600 °C, 1 atm, with S/C=3 and feed flow rate of 100 mL/min. Three channel patterns (i.e., parallel, splitting-jointing and pin-hole) were compared in terms of Figure of Merit (FoM) and specific conversion. Parallel channel design revealed a high value of specific conversion to be about 5.36× 10^{-5} kg_{CH_4}/m^2, while splitting-jointing and pin-hole were 5.33× 10^{-5} and 4.91× 10^{-5}, respectively. Based on FoM, pin-hole design had a high value of 1.34× 10^{-5} $kg_{CH_4}/m^2.Pa$, while the values of splitting-jointing and parallel designs were 0.037× 10^{-5} and 1.28× 10^{-5}, respectively.

1. Introduction

Atmospheric carbon dioxide and pollution are increasing alarmingly due to the burning of fossil fuels. Many scientists attribute global warming to the rising levels of carbon dioxide and other pollutants, some of which pose risks to health, as well. Such risks and hazards can be reduced by using the upgraded and more efficient use of conventional fuels and the by developing non-polluting energy resources. Fuel cells represent a highly efficient and low polluting method for generating electricity and are under development to be applied to both power generation and transport sectors [1].

Solid Oxide Fuel Cells (SOFCs) as energy conversion devices [2] are able to provide highly efficient and clean power for a wide range of small- to large-scale applications. SOFCs are expected to have thermal efficiency of around 50–60 % [3].

As an energy carrier [2], hydrogen (H_2) is

[*]Corresponding author: Irankhah@kashanu.ac.ir

the main feed of SOFC. The H_2 production generally decreases in the following manner: steam reforming, auto-thermal reforming, and partial oxidation [3].

Steam reforming of methane is the dominant and important process of producing syngas and hydrogen [4] and hydrogen production with SOFC cells has attracted significant attention. With cheap hydrogen, troubles and problems associated with energy production and the environment can be solved [5].

For efficient fuel processing of hydrogen for fuel cells, it is important to include a catalyst with high stability and activity and have a reactor with a high surface-to-volume ratio with good thermal efficiency and little dead volumes.

In recent years, micro-reactors are attracting significant attention from pharmaceutical and chemical industries. Such reactors are structurally characterized by inner dimensions in the order of millimeters or smaller. A number of remarkable advantages of micro-structured devices over the conventional chemical reactors have been showcased so far. One of the noticeable advantages of them is the very high area-to-volume ratio that results in considerably improved heat exchange and mass transport rates. However, in several micro-reactor designs, the expected conversion cannot be achieved, which may be attributed to weak mixing of the reactants. Non-uniform distribution of reactants within the micro-channels can cause poor mixing if the design exploits parallel channels [6].

Since the flow in micro-reactors is typically laminar, as a result of the small dimensions, this allows precise computer simulation of the chemical reactions to evaluate strategies to prevail over the aforementioned limitations [7].

Generally, a micro steam reformer is designed with parallel flow channels to make reactant gases flow uniformly. To this end, the channel size, arrangement, and position of inlet and outlet should be appropriately optimized to achieve uniform distribution of the reactant gas [8].

Huang et al. studied the effect of fractal design pattern and gradient catalyst layer on a methanol steam reformer. Relative to a parallel channel design, the CO and methanol conversion ratio of fractal channel design with a uniform catalyst layer can be decreased and increased by 17 % and 8 %, respectively. Moreover, fractal design needs less pumping power [9].

To study the effects of entrance inclination and channel inclination angle on micro-channel steam reforming of methanol, Hao et al. studied a novel channel pattern. The results showed that compared with traditional parallel channels design, the novel design would guarantee flow distribution uniformity and increase the methanol conversion ratio when entrance inclination angle and channel inclination angle were equal to 9° and 55°, respectively [10].

Balaji and Lakshminarayanan investigated a novel design with a configuration of one inlet and two outlets to study flow distribution along the micro-channels for various plate geometries of a micro heat exchanger. They suggested that one inlet/two outlets produced uniform velocities [11].

Pan et al. studied the effect of complex manifold geometries on the micro-channel flow distribution by an analytical model. Results showed that the micro-channel width would dominate the optimization of outlet collecting manifold geometry [12].

An et al. extensively simulated the catalytic combustion for 8 micro-reactor

configurations: oblique fin, wavy serpentine, coiled, pin-hole, coiled with serpentine, and coiled with double serpentine channel geometries. By defining figure of merit (FoM) based on reaction throughput per unit pumping power and catalyst active area, the performance of configurations was compared. The pinhole channel design could ensure the best overall performance over a range of Reynolds numbers studied. The effect was more pronounced at higher Reynolds numbers. It was observed that for each geometry, a higher Reynolds number would result in lower FoM [8].

In the works of An et al. [8] and Arzamendi et al. [13], all the feed entering each reforming channel was supposed to be the same and therefore, the effect of the entrance region was not included in their simulations. Entrance region can impact the uniformity flow through channels. Hence, in the first section of this study, inlet/outlet arrangements for parallel channels are studied in 3 dimensions. Another objective of the current CFD study is to compare new channel designs with the proposed designs of An et al. [8]. The novelty behind this study is that simulations will be carried out in three dimensions which can give a better insight into the design micro-reactors.

2. System description and modeling

2.1. Micro-reformer dimensions and materials

Overall assembly of micro-reformer is shown in Fig. 1. In the middle of two stainless steel casings, a channelized plate on both sides of catalyst was coated and shown in red. As reforming is an endothermic reaction, generally the other side of channel was coupled with an exothermic reaction to supply heat. Since in this assembly all feed passes through all channels, heat must be supplied from the casing outside. One of the advantages of this type of plate and assembly is to study electrophoretic coating method by which both sides can be coated simultaneously.

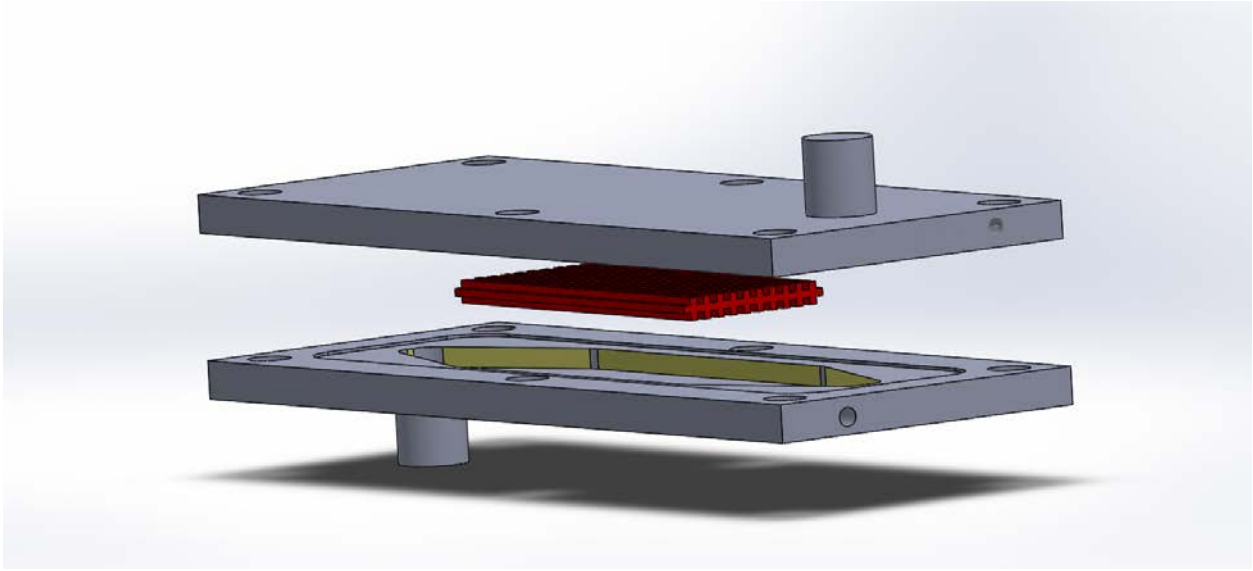

Figure 1. Schematic representation of the micro-reformer, red solid represents coated micro-channel plate mounted into a stainless steel casing.

The reaction takes place on the plate with dimensions of 21×40 mm (Fig. 2). Entrance length of feed is 15 mm and 15 mm for outlet; diameters of inlet/outlet tubes are set to 5

mm. Material of casing and reacting plate is stainless steel 310 so that it can tolerate high temperatures. Typical dimension of 1 mm based on previous researches was selected for channel cross-section [14]. In this study, it is assumed that reactions take place at a constant boundary temperature and heat supplied to micro-reformer through an electrical heat jacket. As illustrated in Fig. 2, both sides of reaction plate have a catalyst-coated surface. In this study, three different designs were investigated for the patterns on the reaction plates, i.e., parallel, splitting-jointing, and pin-hole, as shown in Fig. 3. Parallel channels were typical in micro-reformers and pin-hole pattern was proposed by An et al. [8]; splitting-jointing pattern was a fluid pathway to be compared for the first time. Furthermore, in the case of parallel channels, effect of geometry arrangement of inlet and outlet on the uniformity of velocity distribution was studied.

This type of micro-reformer reactor was under construction to investigate EPD coating method and other parameters as well as variables experimentally.

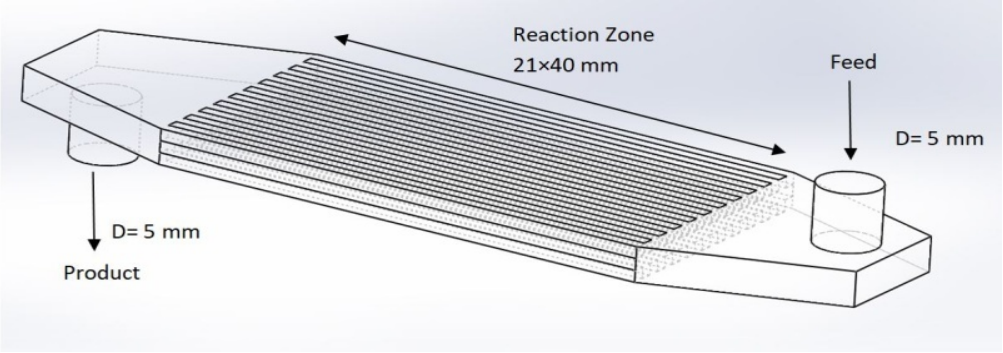

Figure 1. Fluidic and reaction regions of micro-reformer.

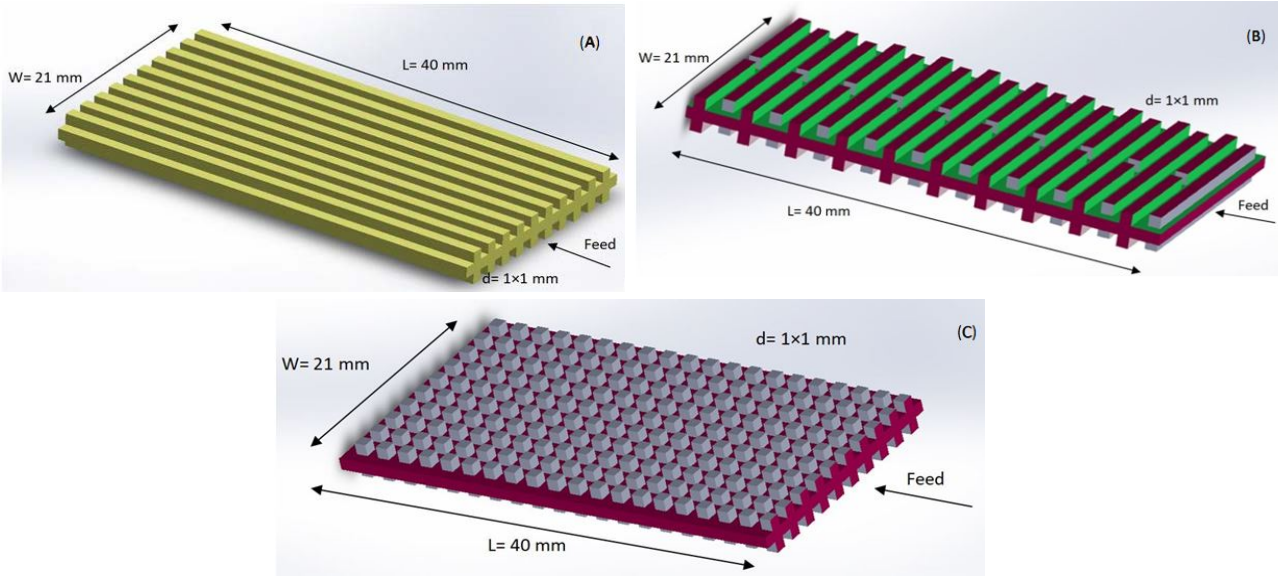

Figure 2. Reaction plate (A) with parallel, (B) splitting-jointing, and (C) pin-hole channels on both sides.

2.2. Modeling

2.2.1. Developing simulation cases

In the first step, geometries were generated using SolidWorks 2014 and then, domains were meshed by applying Gambit 4.2.4. Based on the work of Arzemendi [13],

unstructured meshing was applied. In order to perform the sensitivity analysis of mesh size, hydrogen concentration was chosen. The trend of hydrogen mole concentration in the reactor exit stream is shown in Table 1. The application of almost 8×10^5 mesh was appropriate and further reduction of cell size did not change the simulation outputs significantly.

Table 1
Grid independency check.

Mesh size	H_2 mol % in the outlet
727K	44.2
823K	46.7
931K	47.0
1021K	47.0

Catalytic reactions were modeled considering the micro-channel walls as sources of products and sinks of reactants. A thin and homogeneous monolayer of Ni catalyst was assumed uniformly deposited on walls of channels. Working pressure and temperature were 1 atm and 600 °C, respectively. Maximum calculated value of Reynolds number was around 80; thus, it is expected that flow regime would be laminar. Given that the velocity was lower than sound velocity, it is reasonable to assume that flow was incompressible.

The described structure of the system is a three-dimensional steady-state model.

The governing equations of fluid dynamics are summarized as follows.

The steady-state balance of mass can be expressed as:

$$\frac{\partial(\rho u_x)}{\partial x}+\frac{\partial(\rho u_y)}{\partial y}+\frac{\partial(\rho u_w)}{\partial z}=0 \quad (1)$$

The balance of momentum can be written as:

$$\frac{\partial(\rho u_x u_x)}{\partial x}+\frac{\partial(\rho u_y u_x)}{\partial y}+\frac{\partial(\rho u_z u_x)}{\partial z}+\frac{\partial \tau_{x,x}}{\partial x}+\frac{\partial \tau_{x,y}}{\partial y}+\frac{\partial \tau_{x,z}}{\partial z}+\frac{\partial P}{\partial x}-\rho g=0 \quad (2)$$

$$\frac{\partial(\rho u_x u_y)}{\partial x}+\frac{\partial(\rho u_y u_y)}{\partial y}+\frac{\partial(\rho u_z u_y)}{\partial z}+\frac{\partial \tau_{x,y}}{\partial x}+\frac{\partial \tau_{y,y}}{\partial y}+\frac{\partial \tau_{z,y}}{\partial z}+\frac{\partial P}{\partial y}-\rho g=0 \quad (3)$$

$$\frac{\partial(\rho u_x u_z)}{\partial x}+\frac{\partial(\rho u_y u_z)}{\partial y}+\frac{\partial(\rho u_z u_z)}{\partial z}+\frac{\partial \tau_{x,z}}{\partial x}+\frac{\partial \tau_{y,z}}{\partial y}+\frac{\partial \tau_{z,z}}{\partial z}+\frac{\partial P}{\partial z}-\rho g=0 \quad (4)$$

where

$$\tau_{x,y}=\tau_{y,x}=-\mu\left(\frac{\partial u_x}{\partial y}+\frac{\partial u_y}{\partial x}\right),\ \tau_{y,z}=\tau_{z,y}=-\mu\left(\frac{\partial u_y}{\partial z}+\frac{\partial u_z}{\partial y}\right),\ \tau_{z,x}=\tau_{x,z}=-\mu\left(\frac{\partial u_x}{\partial z}+\frac{\partial u_z}{\partial x}\right) \quad (5)$$

and

$$\tau_{x,x}=-\mu\left(2\frac{\partial u_x}{\partial x}-\frac{2}{3}\Delta.u\right),\ \tau_{y,y}=-\mu\left(2\frac{\partial u_y}{\partial y}-\frac{2}{3}\Delta.u\right),\ \tau_{z,z}=-\mu\left(2\frac{\partial u_z}{\partial z}-\frac{2}{3}\Delta.u\right) \quad (6)$$

For steady-state, incompressible and viscous flow energy equation can be expressed as:

$$\frac{\partial(\rho u_x h)}{\partial x}+\frac{\partial(\rho u_y h)}{\partial y}+\frac{\partial(\rho u_z h)}{\partial x}+\frac{\partial}{\partial x}\left(\rho\sum_{k=1}^{4}w_k h_k u_{k,x}-\lambda_g\frac{\partial T}{\partial x}\right)+\frac{\partial}{\partial y}\left(\rho\sum_{k=1}^{4}w_k h_k u_{k,y}-\lambda_g\frac{\partial T}{\partial y}\right)+$$
$$\frac{\partial}{\partial z}\left(\rho\sum_{k=1}^{4}w_k h_k u_{k,z}-\lambda_g\frac{\partial T}{\partial z}\right)=0 \qquad k=CO_2,\ CO,\ H_2O,\ H_2 \quad (7)$$

The mass balance for species i takes the following form:

$$\rho\left[u_x\frac{\partial w_i}{\partial x}+u_y\frac{\partial w_i}{\partial y}+u_z\frac{\partial w_i}{\partial z}\right]=\rho D_{im}\left[\frac{\partial^2 w_i}{\partial x^2}+\frac{\partial^2 w_i}{\partial y^2}+\frac{\partial^2 w_i}{\partial z^2}\right] \quad (8)$$

where multicomponent diffusion is defined as follows:

$$D_{im}=\frac{1-X_i}{\sum_j\frac{X_i}{D_{ij}}}$$

At the interface between the coated walls and bulk stream, the mass balance for species i is:

$$W_i(s_i)_{interface}+(\rho Y_i u)_{interface}=0$$

$$i=CO_2,CO,H_2O,H_2 \quad (9)$$

s_i is the surface reaction and $s_i=r_i\alpha$. In the next section, r_i is described in detail.

2.2.2. Kinetic rate model

Three main reactions of steam reforming are given below:

$CH_4 + H_2O \leftrightarrow 3\ H_2 + CO\ \Delta H = 206$ kJ/mol — Steam reforming (10)

$CO + H_2O \leftrightarrow H_2 + CO_2\ \Delta H = -41$ kJ/mol — WGS (11)

$CH_4 + 2\ H_2O \leftrightarrow 4\ H_2 + CO_2\ \Delta H = -164$ kJ/mol — Reverse CO_2 methanation (12)

One simple rate equation was applied by Arzemendi [13] in which only partial pressure of methane and temperature affected the rate; however, in this study, the reaction rate expressions of Hou [14] were used where many parameters and variables played roles in the steam reforming rate. These complex rate equations really prolong the simulation run time, but they produce more improved simulation results. The reaction rate expressions are given as follows (Eq. (10)-(12)).

Reaction rates are given in Equations (13)-(15).

$$\mathbf{r_1}=\frac{\mathbf{k_1}\left(\mathbf{P_{CH_4}P_{H_2O}^{0.5}/P_{H_2}^{1.25}}\right)\left(\mathbf{1}-\left(\mathbf{P_{CO}P_{H_2}^3/K_{p1}P_{CH_4}P_{H_2O}}\right)\right)}{(\mathbf{den})^2} \quad (13)$$

$$\mathbf{r_2}=\frac{\mathbf{k_2}\left(\mathbf{P_{CO}P_{H_2O}^{0.5}/P_{H_2}^{0.5}}\right)\left(\mathbf{1}-\left(\mathbf{P_{CO_2}P_{H_2}/K_{p2}P_{CO}P_{H_2O}}\right)\right)}{(\mathbf{den})^2} \quad (14)$$

$$\mathbf{r_3}=\frac{\mathbf{k_3}\left(\mathbf{P_{CH_4}P_{H_2O}/P_{H_2}^{1.75}}\right)\left(\mathbf{1}-\left(\mathbf{P_{CO_2}P_{H_2}^4/K_{p3}P_{CH_4}P_{H_2O}^2}\right)\right)}{(\mathbf{den})^2} \quad (15)$$

$$den=1+K_{CO}P_{CO}+K_{H_2}P_{H_2}^{0.5}+K_{H_2O}\left(P_{H_2O}/P_{H_2}\right)$$

where k_1, k_3 are the reaction rate constants of reactions (10) and (12) in (kmol/ kg_{cat}-s) $(kPa)^{0.25}$, respectively, and k_3 is the reaction rate constant of reaction (11) in (kmol/kg_{cat}-s) (kPa).

K_{p1}, K_{p3} are equilibrium constants of Reactions (10) and (12) in $(kPa)^2$ and K_{p2} is the equilibrium constant of reaction (11). P_i is partial pressure of component i in (kPa). r is the reaction rate in (kmol/ kg_{cat}-s). K_{CO} is the adsorption coefficient of CO in $(kPa)^{-1}$, K_{H_2O} is the adsorption coefficient of H_2O, and $K_{H_2}$is the adsorption coefficient of H_2 in $(kPa)^{-0.5}$. The values of all the mentioned parameters used in simulation are given in Table 2.

Rate equations were introduced to CFD code and as it is a heterogeneous catalytic reaction, loading on the surface is an important factor. As seen in the literature, a catalyst loading of 0.5-8 mg/cm^2 is usually applied [13]. Based on our experiments, almost 4 mg/cm^2 was coated by the EPD coating method, which was accordingly used for simulation purposes.

Table 2
Kinetics parameters; T in Kelvin's degree [14].

Parameter	Value
k_1	$5.922\times10^{8}\exp\left(\frac{-209200}{8.314\,T}\right)$
k_2	$6.028\times10^{-4}\exp\left(\frac{-15400}{8.314\,T}\right)$
k_3	$1.093\times10^{3}\exp\left(\frac{-109400}{8.314\,T}\right)$
K_{p1}	$1.198\times10^{17}\exp\left(\frac{-26830}{8.314\,T}\right)$
K_{p1}	$1.176\times10^{-2}\exp\left(\frac{4400}{8.314\,T}\right)$
K_{p1}	$2.17\times10^{15}\exp\left(\frac{-22430}{8.314\,T}\right)$
K_{co}	$5.127\times10^{-13}\exp\left(\frac{140000}{8.314\,T}\right)$
K_{H_2}	$5.68\times10^{-13}\exp\left(\frac{93400}{8.314\,T}\right)$
K_{H_2O}	$9.251\exp\left(\frac{-15900}{8.314\,T}\right)$

Since hydrogen is needed for the rate equations to be meaningful (partial pressure of H_2 in the denominator of Eq. (13-15)), the small amount of hydrogen was included in the feed so that H_2O:CH_4:H_2=3:1:0.5.

All boundary conditions in the simulation are given in Table 3. Considering specific boundary conditions for each type of micro-reformer, mass, heat, and momentum differential equations were solved iteratively until the convergence criterion was satisfied. Solution method was SIMPLE and criterion of convergence was set equal to absolute residual of 1×10^{-6}.

Simulations were performed by commercial ANSYS FLUENT 17 software on a HP EliteBook 840 workstation running MS-Windows 10® ×64 with an available RAM of 8 GB.

3. Results and discussion

3.1. Inlet/outlet arrangement

To optimize feed and product stream positions (inlet/outlet), parallel channel case was analyzed. For a better visual understanding of velocity distribution, cross sectional view of channels was numbered according to Fig. 4. In terms of fluid mechanics, velocities grow through channels till they get fully developed and then continue unchanged. Typically a fully developed region is obtained in channels and then, stream passes a length which is five times the hydraulic diameter of the channel. Hence in our study velocities were compared in the center length of micro-channels to be ensured fully developed criteria was obtained.

Table 3
Operating and boundary conditions.

Steam to carbon ratio(S/C)	3
Pressure	101.3 kPa
Feed temperature	600 °C
Feed flow rate	100 mL/min (STP)
Feed composition	H_2O:CH_4:H_2=3:1:0.5
T_w	600 °C

Fig. 5(A)–(D) represent four types of configurations for investigation of velocity distribution across channels. Velocity distribution of these configurations is shown in Fig. 6; based on this figure and calculated standard deviations (σ), (A= 0.00405 m/s, B= 0.00409 m/s, C= 0.00378 m/s, and D=0.00327 m/s), it can be concluded that one inlet/two outlets (D) arrangement on the opposite sides is the best among other arrangements since it has the lowest σ. It is shown that two outlets give better dispersion and distribution [9, 11]. The result obtained is in agreement with that of Balaji [10]. In the

current design and geometry, it was supposed that the two sides of reaction plate were active and then to include symmetry in flow path, it is necessary to include outlet and inlet on the opposite sides.

Some channels exhibit different behaviors in small amount from the others and this behavior originates from the fact that feed entrance regime of micro-reformer is somehow turbulent.

The results obtained are of course useful for designing integrated micro-reformers, where outside of reforming body, hot fluid passes the exchange heat. Having uniform velocity distribution gives uniform conversion and prohibits hot/cold spots along reforming. Appearing hot/cold spot on the casing may apply thermal stress to the micro-reformer body and lead to its deformation, which may cause leakage after some periods of working.

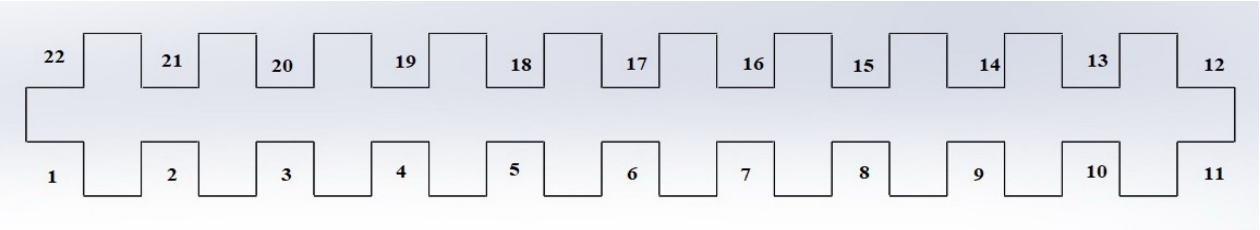

Figure 3. Numbering and cross section view of channels.

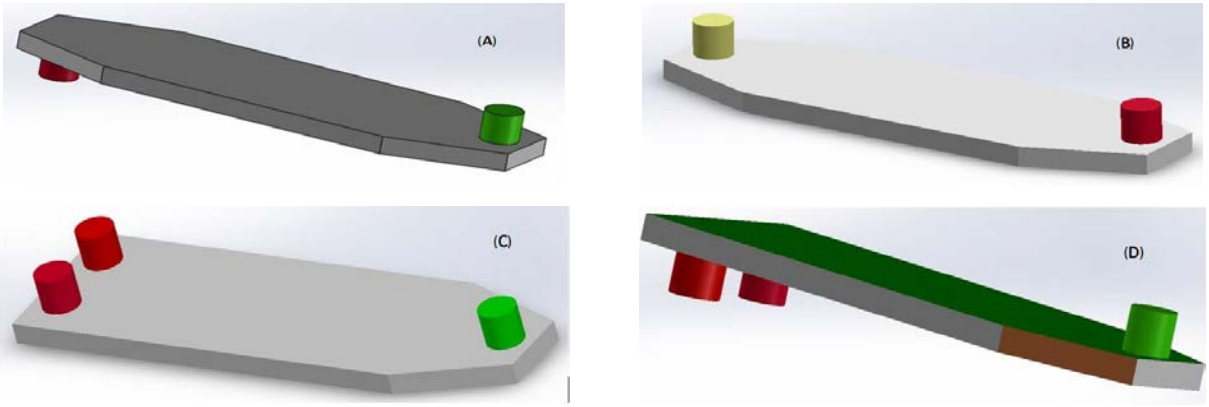

Figure 4. Inlet/outlet configurations: (A) one inlet/one outlet on the opposite sides, (B) one inlet/one outlet on the same sides, (C) one inlet/two outlets on the same sides, and (D) one inlet/two outlets on the opposite sides.

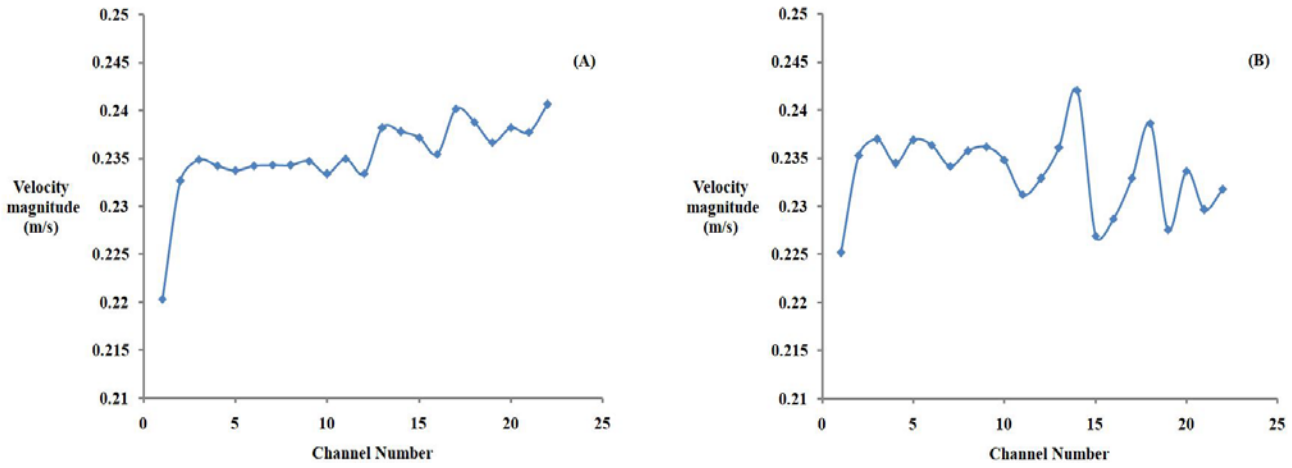

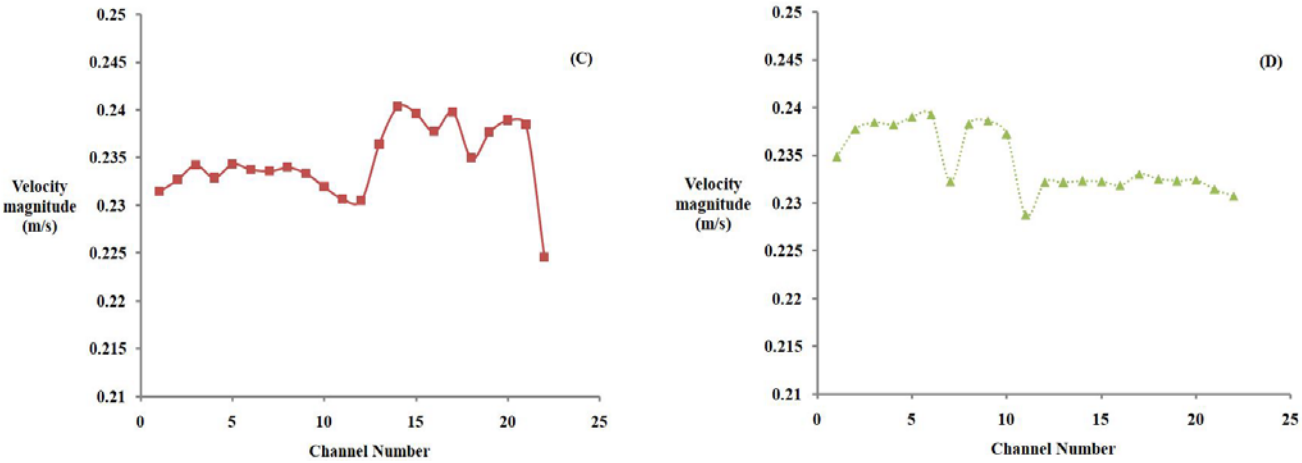

Figure 5. Velocity distribution across channels, S/C=3, H_2O:CH_4:H2=3:1:0.5; $\dot{m}=1\times10^{-6}$ kg/s.

3.2. Channel design

In order to compare channel design of reaction plates, the three mentioned reaction plates (Fig. 3) were simulated. Figure of merit (FoM) is the criterion for comparison of channel types based on the findings of An et al. [8]. FoM is defined such that it can include all the costs (surface area, pressure drop) and the benefit (methane conversion) of reforming as follows:

$$\mathrm{FoM} = \frac{\dot{m}_{r,in} - \dot{m}_{r,out}}{A_{wall} P_{pump}} \quad (16)$$

where m, P_{pump}, and A_{wall} are the mass flow rate, pumping power, and coated catalytic surface area, respectively. Pumping power is related to flow rate and pressure drop ($P_{pump}=Q\times\Delta P$). At a given flow rate, pumping power corresponds to pressure drop [7]. However, for typical flow rates of these micro-reformers, pressure drop through reaction plate is at most lower than 200 Pa. Since the inlet feed pressure (methane and steam) is almost 100 kPa, it seems that pressure drop does not play a significant role in the economy of fuel cell integrated plant. Pressure and pressure drop gain siginificance in case of separating micro-reformer products by a membrane; therefore, another criterion emerges out to show micro-reformer performance. The new criterion is specific conversion which is the ratio of mass consumption per catalytic surface area.

In Fig. 7, contours of methane mole fraction for three reaction plates are illustrated. The contours are at a level of 0.5 mm from middle of the plates. For parallel channel design (Fig. 7A), it is obvious that dead volumes do not appear along the channels, but as shown in Fig. 7B and C, for pin-hole design, dead volumes exist in small areas among pins as well as for the corners of splitting-jointing design.

Further, in Fig. 8, counters of hydrogen are shown. Like methane consumption, the same pattern is seen for hydrogen production.

(A)

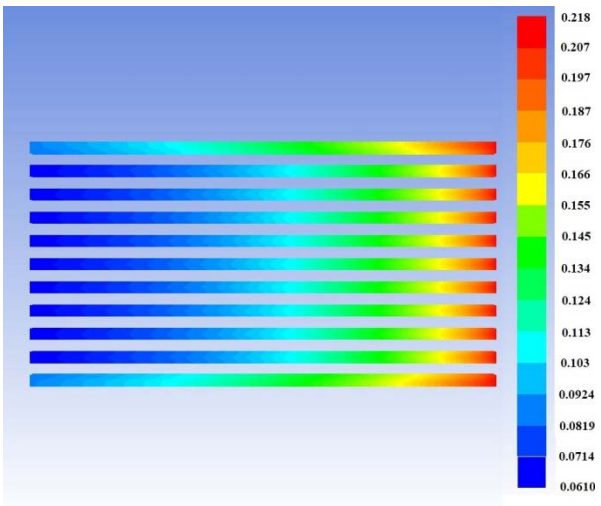

(B)

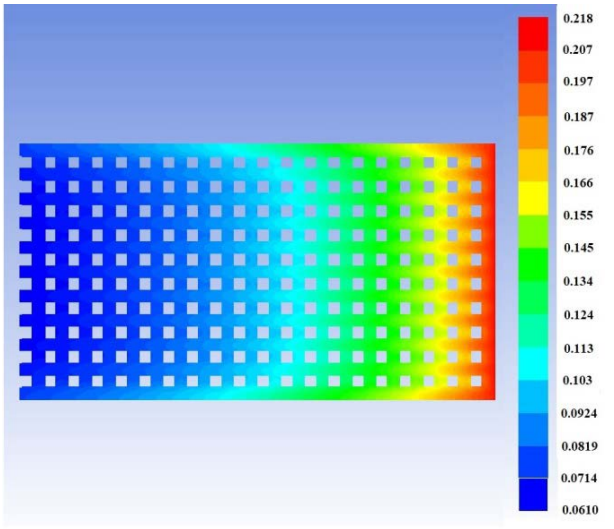

(C)

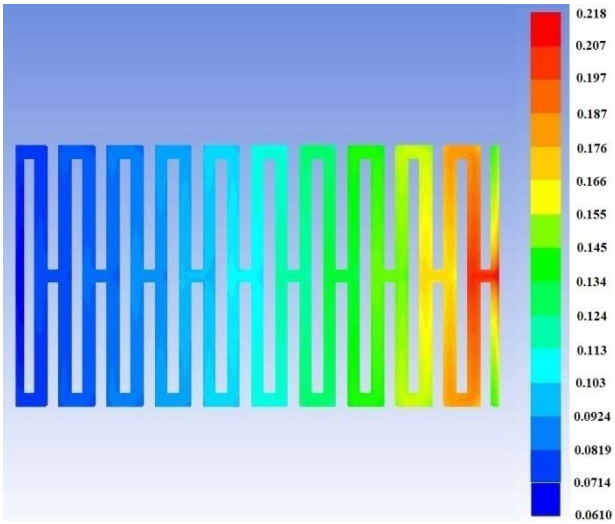

Figure 6. 2D view of CH_4 mole fraction at z=0.5 mm for (A) parallel, (B), pin-hole and (C) splitting-jointing channels.

(A)

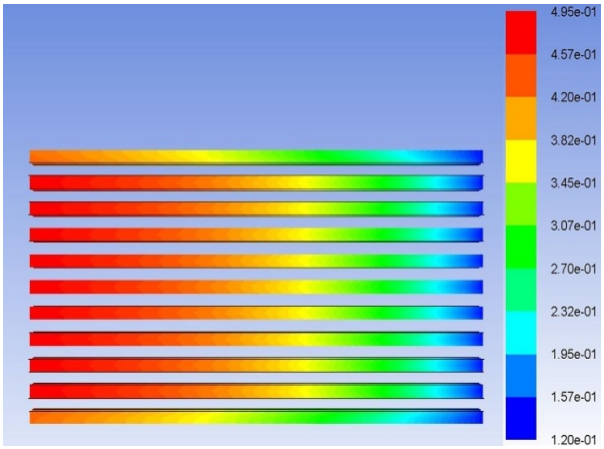

(B)

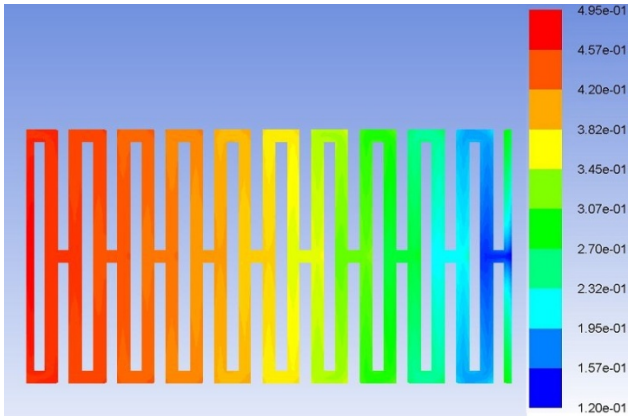

(C)

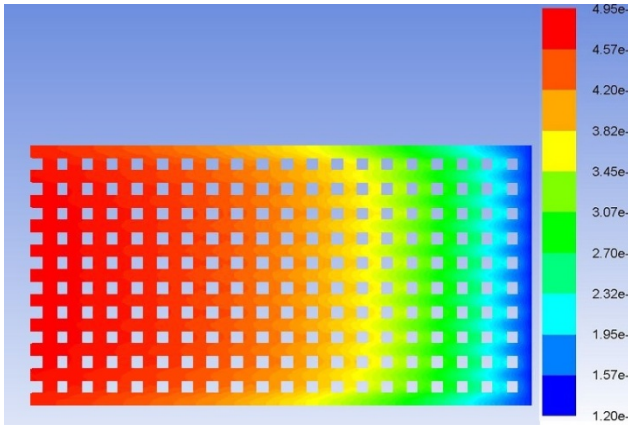

Figure 7. 2D view of H_2 mole fraction at z=0.5 mm for (A) parallel, (B), pin-hole and (C) splitting-jointing channels.

In order to compare designs, specific CH_4 conversion was selected (Table 4). If FoM was chosen as a comparison base, the pin-hole design would have a higher FoM value. According to Table 4, since the pressure drop of splitting-jointing design is the highest, it has the lowest FoM. The pressure drop comes from the fact that cross area for flowing materials is just 1 mm^2; thus, Reynolds number increases and then pressure drops strongly. However, regarding specific conversion, i.e. neglecting pressure drop, parallel design is characterized by a high value. In the parallel design, we have a bit dead volume and the entire catalytic coated surface is available for reactants. However, in other designs, there are some dead zones in

which mass transfer rate inside these zones are low because mass transfer is controlled strongly by diffusion with respect to convection.

Table 4
Reaction plate design comparison; S/C=3; Feed=1×10^{-6} kg.s^{-1}; $H_2O:CH_4:H_2$=3:1:0.5; Pressure=101.3 kPa; Temperature= 600 °C.

Plate type	Reaction area (mm^2)	Pressure drop (Pa)	FoM $(kg_{CH_4}/m^2.Pa)\times10^5$	Specific conversion $(kg_{CH_4}/m^2)\times10^5$
Parallel	2480	1.4	1.28	5.36
Splitting-jointing	2540	70.4	0.037	5.33
Pin-hole	2860	1.8	1.34	4.91

4. Conclusions

New reaction plate and assembly for steam micro-reformer were presented. This assembly was suitable for studying EPD coating method in which both sides of the plate were involved in catalytic reaction. This micro-reformer was constructed and coating methods were studied, the results of which will be published soon. In this work, a CFD analysis was performed to study inlet/outlet arrangement for micro-reformer in which reaction took place on both sides. A dimension of 1×1 mm was selected for channels and one reaction plate was 21×20 mm^2. Regarding feed and product arrangements, one inlet and two outlets on opposite sides give the velocity distribution more uniformly than other arrangements. Again, in terms of FoM and specific conversion, three channel designs, i.e., parallel, splitting-jointing, and pin-hole, were compared on two reaction plates with 21×40 mm^2 dimension, where steam reforming took place on both sides. If pressure drop along micro-reformer was considered an important factor in fuel-processing plant design, pin-hole design would give a higher FoM value than other designs; however, regarding specific conversion value, parallel design led to a value of specific conversion more than other designs.

Nomenclature

ΔH	heat of reaction.
D_{im}	multicomponent diffusion coefficient of species i through the mixture.
D_{ij}	binary diffusion coefficient i into species j.
k_i	reaction rate constant i=1,2,3.
K_i	adsorption coefficient of species i.
K_{pi}	equilibrium constant of reaction i.
k	thermal diffusivity.
P	pressure.
P_i	partial pressure of species i.
R	ideal gas constant.
r	reaction rate.
T	temperature.
T_w	casing body wall temperature.
u	velocity vector.
W	molecular weight.
Y	mass fraction.
x,y,z	Cartesian coordinates.
X_i	mole fraction of species i.
Greek symbols	
α	deposited catalyst loading.
ρ	fluid density.
$\tau_{i,i}$	shear stress.
$\tau_{i,j}$	normal stress.
Δ	gradient vector.
μ	viscosity.
λ_g	thermal conductivity.

References

[1] Adams, V. W., "The potential of fuel cells to reduce energy demands and pollution from the UK transport sector", Ph. D. Thesis, Open University, (1998).

[2] Dixit, M., Baruah, R., Parikh, D., Sharma, S. and Bhargav, A., "Autothermal reforming of methane on rhodium catalysts: microkinetic analysis for model reduction", *Computers and Chemical Engineering*, **89**, 149 (2016). (http://doi.org/10.1016/j.compchemeng.2016.03.032).

[3] Lee, T. S., Chung, J. N. and Chen, Y. –C., "Design and optimization of a combined fuel reforming and solid oxide fuel cell system with anode off-gas recycling", *Energy Conversion and Management*, **52**, 3214 (2011).

[4] Kumar, A., Baldea, M. and Edgar, T. F., "A physics-based model for industrial steam-methane reformer optimization with non-uniform temperature field", *Computers and Chemical Engineering*, **105**, 224 (2017). (http://doi.org/10.1016/j.compchemeng.2017.01.002).

[5] Liu, C. –J., Ye, J., Jiang, J. and Pan, Y., "Progresses in the preparation of coke resistant Ni-based catalyst for steam and CO_2 reforming of methane", *Chemical Catalyst Chemistry*, **3**, 529 (2011).

[6] Rebrov, E. V., Schouten, J. C. and de Croon, M. H. J. M., "Single-phase fluid flow distribution and heat transfer in microstructured reactors", *Chem. Eng. Sci.*, **66**, 1374 (2011).

[7] Watts, P. and Haswell, S. J., "The application of micro-reactors for small scale organic synthesis", *Chemical Engineering Technology*, **28** (3), 290 (2005).

[8] An, H., Li, A., Sasmito, A. P., Kurnia, J. C., Jangam, S. V. and Mujumdar, A. S., "Computational fluid dynamics (CFD) analysis of micro-reactor performance: Effect of various configurations", *Chemical Engineering Science*, **75**, 85 (2012).

[9] Huang, Y. -X., Jang, J. –Y. and Cheng, C. –H., "Fractal channel design in a micro methanol steam reformer", *International Journal of Hydrogen Energy*, **39**, 1998 (2014).

[10] Hao, Y. H., Du, X. Z., Yang, L. J., Shen, Y. .G and Yang, Y. P., "Numerical simulation of configuration and catalyst-layer effects on micro-channel steam reforming of methanol", *International Journal of Hydrogen Energy*, **36**, 15611 (2011).

[11] Balaji, S. and Lakshminarayanan, S., "Improved design of micro-channel plate geometry for uniform flow distribution", *Canadian Journal of Chemical Engineering*, **84**, 715 (2006).

[12] Pan, M., Tang, Y., Pan, L. and Lu, L., "Optimal design of complex manifold geometries for uniform flow distribution between micro-channels", *Chemical Engineering Journal*, **137**, 339 (2008).

[13] Arzamendi, G., Diéguez, P. M., Montes, M., Odriozola, J. A., Falabella Sousa-Aguiar, E. and Gandía, L. M., "Methane steam reforming in a micro-channel reactor for GTL intensification: A computational fluid dynamics simulation study", *Chemical Engineering Journal*, **154**, 168 (2009).

[14] Hou, K. and Hughes, R., "The kinetics of methane steam reforming over Ni/α-Al_2O_3 catalyst", *Chemical Engineering Journal*, **82**, 311 (2001).